Adaptive Nonlinear Guidance Law Considering Control Loop Dynamics

DONGKYOUNG CHWA, Member, IEEE
JIN YOUNG CHOI, Member, IEEE
Seoul National University
Korea

A new adaptive nonlinear guidance law is proposed here. The fourth order state equation for integrated guidance and control loop is formulated taking into consideration the target uncertainties and control loop dynamics. The state equation is further changed into the normal form by nonlinear coordinate transformation. Using the normal form of state equation, an adaptive nonlinear guidance law is proposed to compensate for the uncertainties in both target acceleration and control loop dynamics. The proposed law adopts the sliding mode control approach with adaptation for unknown bound of uncertainties. The present approach can effectively solve the existing guidance problem against target maneuver and the limited performance of control loop. We have provided the stability analyses and performed simulations comparing favorably our approach to the state of the art.

Manuscript received March 12. 2001; revised June 9, 2003; released for publication July16, 2003.

IEEE Log No. T-AES/39/4/822046.

Refereeing of this contribution was handled by J. L. Leva.

This research was supported by the Agency for Defense Development and the Automatic Control Research Center of Seoul National University.

Authors' address: School of Electrical Engineering, Seoul National University, Kwanak PO Box 34, Seoul 151-742, Korea, E-mail: (jychoi@ee.snu.ac.kr).

0018-9251/03/$17.00 © 2003 IEEE

I. INTRODUCTION

In the guidance area [1, 2], there has been research on proportional navigation (PN) [3], true proportional navigation (TPN) [4], augmented proportional navigation (APN) [5, 6], optimal guidance law (OGL) [7–14], ideal proportional navigation (IPN) [15], generalized true proportional navigation (GTPN) [16, 17], and realistic true proportional navigation (RTPN) [18, 19]. In particular, although PN is quite simple to implement and is also known to be an optimal algorithm for a nonmaneuvering target, its performance is degraded with target maneuvering and it may be ineffective for some orientations between missile and target. The PN-variant guidance algorithms such as OGL and APN require information about target acceleration, missile velocity change, and missile acceleration. Although the information can be measured or estimated more accurately with the development of sensors and estimators, the complexity and the cost of the guidance system increase and the uncertainties or errors in these values prevent the expected performance. In practice, as target acceleration can change rapidly, the guidance law using this information may be quite restrictive in that it is difficult to obtain the information without time delay.

More recently, nonlinear control theories have been employed in guidance law using the Lyapunov method [20], nonlinear geometric method [21–23], nonlinear H_∞ method [24], and sliding mode control method [25–27]. In particular, the sliding mode guidance law assumes that the upper bound of target acceleration is known. Since the bound of uncertainty may be unknown, we may have to assume a conservative one and performance in the guidance system might be degraded accordingly.

Furthermore, all of the above guidance laws are designed with the assumption that the response of the control system is ideal or similar to a low pass filter [11–14]. In an actual situation, due to flight conditions and unexpected environments, we cannot expect the ideal performance of the control system. Since the guidance system is designed without addressing this situation, the discrepancy between the ideal control system and the actual one can lead to the unsatisfactory performance. To improve performance, [28–30] suggest the simultaneous design of the guidance and control loop, i.e., the integrated missile guidance and control system. This method adopts the optimal control technique together with the gain scheduling approach. It requires a large amount of computation and memory for a highly agile target maneuver.

We propose another design approach for integrated guidance and control. The integrated guidance and control loop is formulated by a nonlinear state

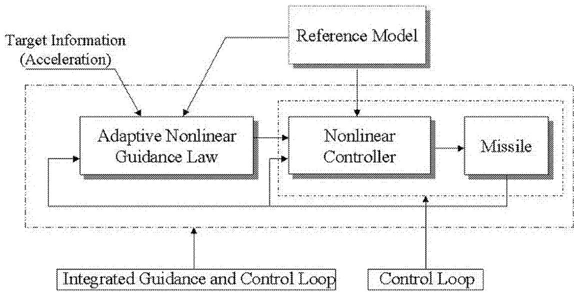

Fig. 1. Approach to guidance and control for the missile using adaptive technique.

equation, which is valid for all flight conditions. The integrated dynamic equation includes uncertainties in both control loop dynamics and target acceleration. This equation is further changed into normal form by coordinate transformation. For the normal form equation, an adaptive nonlinear guidance law is derived using the sliding mode control theory together with parameter adaptation to compensate for the uncertainties. We analyze the stability of the integrated guidance and control loop, and also evaluate the performance through simulations for actual missile model [31] to show the effectiveness of our approach.

The rest of this paper is organized as follows. Section II describes the modeling of integrated guidance and control loop. In Section III, an adaptive nonlinear guidance law considering target uncertainties and the control loop dynamics is presented and also stability of the resulting overall missile system is analyzed. Section IV shows the simulation results for the proposed adaptive nonlinear guidance method. The conclusions are given in Section V.

II. MODELING OF INTEGRATED GUIDANCE AND CONTROL LOOP

In this section, an integrated model for guidance and control loop is formulated. Our approach to an integrated guidance and control is depicted in Fig. 1. The control loop consists of a missile system and a nonlinear controller, and is designed so that the control loop follow a given reference model. The adaptive nonlinear guidance law considers uncertainties in both target acceleration and control loop dynamics. Thus, the overall system leads to an integrated guidance and control loop.

The authors have proposed the nonlinear control scheme for the skid-to-turn (STT) missiles [31]. Here, we utilize the scheme for control loop. The control loop is briefly described in the following. By assumptions usually made in the design of missile control system and also applying the functional approximation technique, we can have the yaw dynamics given by

$$\begin{cases} \dot{\beta} = -r + \dfrac{QS}{Um}(w_{y1}\beta + w_{y2}\beta^3 + w_{y3}\delta_r + \Delta_y) \\ \dot{r} = -Q(v_{a1}\beta + v_{a2}\beta^3 + \Delta_a) - \dfrac{QS(l_f - l_g)}{I_M} \\ \qquad \times (w_{y1}\beta + w_{y2}\beta^3 + w_{y3}\delta_r + \Delta_y) \\ a_m = \dfrac{QS}{m}(w_{y1}\beta + w_{y2}\beta^3 + w_{y3}\delta_r + \Delta_y) \end{cases} \tag{1}$$

where β is side-slip angle; r is yaw angular rate; δ_r is deflection of yaw control fin; Q is dynamic pressure; S is aerodynamic reference area; $I_M = I_z$ is moment of inertia about z-axis; m is missile mass; l_f and l_g are distances from the nose of a missile to the center-of-pressure of control fins and the center-of-gravity; a_m is acceleration output; w_{y1}, w_{y2}, w_{y3}, v_{a1}, v_{a2} are slowly time-varying parameters depending on Mach number and bank angle ϕ_A, defined by $w_{yj} = \sum_{i=1}^{N}\mu_i(M_m)(c_{ij}^{f1} + c_{ij}^{f2}\sin^2(2\phi_A))$, $v_{a1} = c_{a1} + c_{a2}|\phi_A|$, $v_{a2} = c_{a3}$, $\mu_i(M_m) = \mu_i^0(M_m)/\sum_{j=1}^{N}\mu_j^0(M_m)$, $\mu_i^0(M_m) = \exp(-(M_m - M_i)^2/\sigma_i^2)$ for $i = 1,\ldots,N$ and $j = 1,2,3$; c_{ij}^{f1}, c_{ij}^{f2}, c_{a1}, c_{a2}, c_{a3} are all fitting parameters obtained by a curve fitting technique from a look-up table of aerodynamic coefficients for $M_m = M_i$; and Δ_y and Δ_a are approximation errors. In order to make the above system almost linear, we employ the control input

$$\delta_r = \frac{1}{w_{y3}}\left(\frac{m(u_y + Ur)}{QS} - w_{y1}\beta - w_{y2}\beta^3\right) \tag{2a}$$

$$u_y = -\frac{Uh_v u_1}{Q(v_{a1} + 3v_{a2}\beta^2)} \tag{2b}$$

$$\dot{u}_1 = -2\omega_n\xi u_1 + \omega_n^2(a_{mc} - a_m) \tag{2c}$$

where a_{mc} is acceleration command from the guidance loop. The control input (2) makes the overall control loop follow a second-order reference model

$$\ddot{a}_m + 2\xi\omega_n a_m + \omega_n^2 a_m = \omega_n^2 a_{mc} + \Delta_c \tag{3}$$

where Δ_c is an uncertainty arising from the missile uncertainty Δ_y and Δ_a. For details about the control loop, see [31]. Equation (4) can be expressed in state space form as

$$\begin{aligned} \dot{X}_c &= \begin{pmatrix} 0 & 1 \\ -a_{c1} & -a_{c2} \end{pmatrix} X_c + \begin{pmatrix} 0 \\ b_c \end{pmatrix} u_c + \begin{pmatrix} 0 \\ \Delta_c \end{pmatrix} \\ &=: A_c X_c + B_c u_c + D_c \end{aligned} \tag{4}$$

where $X_c = (x_{c1}\ \ x_{c2})^T = (a_m\ \ \dot{a}_m)^T$, $a_{c1} = \omega_n^2$, $a_{c2} = 2\xi\omega_n$, $b_c = \omega_n^2$, $u_c = a_{mc}$, and ξ and ω_n are design parameters of the control loop.

In the following, an integrated model of a guidance loop including the control loop dynamics (4) is formulated. For convenience, a guidance problem in three-dimensional space is considered as the following two-dimensional guidance problems: the projected horizontal plane (X_r-Y_r plane) and the projected vertical plane (X_r-Z_r plane) where (X_r, Y_r, Z_r) denotes the inertial reference coordinate system. The simultaneous intercepts on both planes imply the true intercept in the original three-dimensional space. In each plane, the missile-target interception can be characterized by two variables: the missile-target range R and the line-of-sight (LOS) angle σ, which are relative measures to their fixed reference frames. In the PN law, the acceleration commands are generated in the direction of making the rate of rotation of the LOS $\dot{\sigma}$ be equal to zero.

As σ is a small value, it can be defined as

$$\sigma = \frac{l}{R} \tag{5}$$

where l is a projected y-component of R. Differentiating (5), we can get

$$\dot{\sigma} = \frac{\dot{l}R - l\dot{R}}{R^2} \tag{6}$$

$$\begin{aligned}
\ddot{\sigma} &= \frac{\ddot{l}R - l\ddot{R}}{R^2} - \frac{(l\dot{R} + \dot{l}R)R^2 - 2lR\dot{R}^2}{R^4} \\
&= \frac{\ddot{l}}{R} - \frac{2\dot{l}\dot{R}}{R^2} - \frac{l\ddot{R}}{R^2} + \frac{2l\dot{R}^2}{R^3} \\
&= \frac{\ddot{l}}{R} - \frac{l\ddot{R}}{R^2} - \frac{2\dot{R}}{R}\left(\frac{\dot{l}R - l\dot{R}}{R^2}\right) \\
&= \frac{1}{R}(-a_m + a_T) - \frac{\ddot{R}}{R}\sigma - \frac{2\dot{R}}{R}\dot{\sigma}
\end{aligned} \tag{7}$$

where a_T is target acceleration.

Defining the state $X_g = (x_{g1} \ \ x_{g2})^T = (\sigma \ \ \dot{\sigma})^T$ in (7), the state equation of the guidance loop is expressed by

$$\begin{aligned}
\dot{X}_g &= \begin{pmatrix} 0 & 1 \\ -a_{g1}(t) & -a_{g2}(t) \end{pmatrix} X_g + \begin{pmatrix} 0 \\ -b_g(t) \end{pmatrix} a_m + \begin{pmatrix} 0 \\ b_g(t) \end{pmatrix} a_T \\
&=: A_g X_g + B_g u_g + D_g
\end{aligned} \tag{8}$$

where $a_{g1}(t) = \ddot{R}(t)/R(t)$, $a_{g2}(t) = 2\dot{R}(t)/R(t)$, $b_g(t) = 1/R(t)$, $u_g = a_m$, and $\dot{R}$ is the relative velocity between the target and the missile. Since from (4) $u_g = x_{c1} = C_g X_c = [1 \ \ 0]X_c$ holds, the guidance loop (8) and the control loop (4) can be combined as

$$\begin{aligned}
\dot{X}_{igc} &= \begin{pmatrix} A_g & B_g C_g \\ 0 & A_c \end{pmatrix} X_{igc} + \begin{pmatrix} 0 \\ B_c \end{pmatrix} u_c + \begin{pmatrix} D_g \\ D_c \end{pmatrix} \\
&= A_{igc} X_{igc} + B_{igc} u_c + D_{igc}
\end{aligned} \tag{9a}$$

$$\begin{aligned}
Y_{igc} &= x_{g2} \\
&= C_{igc} X_{igc}
\end{aligned} \tag{9b}$$

where

$$X_{igc} = \begin{pmatrix} X_g \\ X_c \end{pmatrix}, \qquad A_{igc} = \begin{pmatrix} 0 & 1 & 0 & 0 \\ -a_{g1} & -a_{g2} & -b_g & 0 \\ 0 & 0 & 0 & 1 \\ 0 & 0 & -a_{c1} & -a_{c2} \end{pmatrix}$$

$$B_{igc} = (0 \ \ 0 \ \ 0 \ \ b_c)^T, \qquad C_{igc} = (0 \ \ 1 \ \ 0 \ \ 0)$$

$$D_{igc} = (0 \ \ b_g a_T \ \ 0 \ \ \Delta_c)^T.$$

The guidance law aims to find the acceleration command corresponding to the input variable (i.e., u_c) so that the LOS rate converges to zero. The above equation for the integrated guidance and control loop contains uncertainties in both the target and control loop. Thus, the guidance law is designed to compensate for these uncertainties. To apply nonlinear control theory to the integrated guidance and control loop, the state equation (9) must be transformed into normal form. The output is chosen by

$$y = Y_{igc} =: x_1. \tag{10}$$

Differentiating the output, we have

$$\begin{aligned}
\dot{x}_1 &= -a_{g1}x_{g1} - a_{g2}x_1 - b_g x_{c1} + b_g a_T \\
&= x_2 + \bar{\Delta}_1
\end{aligned} \tag{11}$$

where

$$x_2 = -a_{g1}x_{g1} - a_{g2}x_1 - b_g x_{c1}, \qquad \bar{\Delta}_1 = b_g a_T. \tag{12}$$

Differentiation yields

$$\begin{aligned}
\dot{x}_2 &= -\dot{a}_{g1}x_{g1} - a_{g1}\dot{x}_{g1} - \dot{a}_{g2}x_1 - a_{g2}\dot{x}_1 - \dot{b}_g x_{c1} - b_g \dot{x}_{c1} \\
&= -\dot{a}_{g1}x_{g1} - a_{g1}x_1 - \dot{a}_{g2}x_1 - a_{g2}x_2 - a_{g2}\bar{\Delta}_1 - \dot{b}_g x_{c1} - b_g x_{c2} \\
&= -(a_{g1} + \dot{a}_{g2})x_1 - a_{g2}x_2 - \dot{a}_{g1}x_{g1} - \dot{b}_g x_{c1} - b_g x_{c2} - a_{g2}\bar{\Delta}_1 \\
&= x_3 + \bar{\Delta}_2
\end{aligned} \tag{13}$$

where

$$\begin{aligned}
x_3 &= -(a_{g1} + \dot{a}_{g2})x_1 - a_{g2}x_2 - \dot{a}_{g1}x_{g1} - \dot{b}_g x_{c1} - b_g x_{c2} \\
\bar{\Delta}_2 &= -a_{g2}\bar{\Delta}_1.
\end{aligned} \tag{14}$$

Similarly, we have

$$\begin{aligned}
\dot{x}_3 &= -(\dot{a}_{g1} + \ddot{a}_{g2})x_1 - (a_{g1} + \dot{a}_{g2})\dot{x}_1 - \dot{a}_{g2}x_2 - a_{g2}\dot{x}_2 \\
&\quad - \ddot{a}_{g1}x_{g1} - \dot{a}_{g1}\dot{x}_{g1} - \ddot{b}_g x_{c1} - \dot{b}_g \dot{x}_{c1} - \dot{b}_g x_{c2} - b_g \dot{x}_{c2} \\
&= -(\dot{a}_{g1} + \ddot{a}_{g2})x_1 - (a_{g1} + \dot{a}_{g2})x_2 - (a_{g1} + \dot{a}_{g2})\bar{\Delta}_1 \\
&\quad - \dot{a}_{g2}x_2 - a_{g2}x_3 - a_{g2}\bar{\Delta}_2 - \ddot{a}_{g1}x_{g1} - \dot{a}_{g1}x_1 - \ddot{b}_g x_{c1} \\
&\quad - 2\dot{b}_g x_{c2} - b_g(-a_{c1}x_{c1} - a_{c2}x_{c2} + b_c u_c + \Delta_c) \\
&= -(2\dot{a}_{g1} + \ddot{a}_{g2})x_1 - (a_{g1} + 2\dot{a}_{g2})x_2 - a_{g2}x_3 - \ddot{a}_{g1}x_{g1} \\
&\quad + (-\ddot{b}_g + b_g a_{c1})x_{c1} + (-2\dot{b}_g + b_g a_{c2})x_{c2} \\
&\quad - b_g b_c u_c + \bar{\Delta}_3
\end{aligned} \tag{15}$$

where

$$\bar{\Delta}_3 = -(a_{g1} + \dot{a}_{g2})\bar{\Delta}_1 - a_{g2}\bar{\Delta}_2 - b_g\Delta_c. \tag{16}$$

Letting the state variable $x_4 = x_{g1}$, x_{c1} and x_{c2} can be expressed in terms of x_1, x_2, x_3, and x_4 as follows

$$\begin{aligned} x_{c1} &= -\frac{1}{b_g}(x_2 + a_{g1}x_{g1} + a_{g2}x_1) \\ &= -\frac{a_{g2}}{b_g}x_1 - \frac{1}{b_g}x_2 - \frac{a_{g1}}{b_g}x_4 \end{aligned} \tag{17}$$

$$\begin{aligned} x_{c2} &= -\frac{1}{b_g}\{x_3 + (a_{g1} + \dot{a}_{g2})x_1 + a_{g2}x_2 + \dot{a}_{g1}x_{g1} + \dot{b}_g x_{c1}\} \\ &= \left(-\frac{a_{g1} + \dot{a}_{g2}}{b_g} + \frac{a_{g2}\dot{b}_g}{b_g^2}\right)x_1 + \left(-\frac{a_{g2}}{b_g} + \frac{\dot{b}_g}{b_g^2}\right)x_2 \\ &\quad + \left(-\frac{1}{b_g}\right)x_3 + \left(-\frac{\dot{a}_{g1}}{b_g} + \frac{a_{g1}\dot{b}_g}{b_g^2}\right)x_4. \end{aligned} \tag{18}$$

Using the above expression of x_{c1} and x_{c2}, we have

$$\dot{x}_3 = a_1x_1 + a_2x_2 + a_3x_3 + a_4x_4 - b_gb_cu_c + \bar{\Delta}_3 \tag{19}$$

where

$$\begin{aligned} a_1 &= -(2\dot{a}_{g1} + \ddot{a}_{g2}) + \frac{(\ddot{b}_g - b_ga_{c1})a_{g2}}{b_g} \\ &\quad + (2\dot{b}_g - b_ga_{c2})\left(\frac{a_{g1} + \dot{a}_{g2}}{b_g} - \frac{a_{g2}\dot{b}_g}{b_g^2}\right) \end{aligned} \tag{20}$$

$$\begin{aligned} a_2 &= -(a_{g1} + 2\dot{a}_{g2}) + \frac{\ddot{b}_g - b_ga_{c1}}{b_g} \\ &\quad + (2\dot{b}_g - b_ga_{c2})\left(\frac{a_{g2}}{b_g} - \frac{\dot{b}_g}{b_g^2}\right) \end{aligned} \tag{21}$$

$$a_3 = -a_{g2} + \frac{2\dot{b}_g - b_ga_{c2}}{b_g} \tag{22}$$

$$\begin{aligned} a_4 &= -\ddot{a}_{g1} + \frac{(\ddot{b}_g - b_ga_{c1})a_{g1}}{b_g} \\ &\quad + (2\dot{b}_g - b_ga_{c2})\left(\frac{\dot{a}_{g1}}{b_g} - \frac{a_{g1}\dot{b}_g}{b_g^2}\right). \end{aligned} \tag{23}$$

Thus, denoting $x_0 = [x_1\ \ x_2\ \ x_3\ \ x_4]^T$, we have

$$\dot{x}_0 = \begin{pmatrix} 0 & 1 & 0 & 0 \\ 0 & 0 & 1 & 0 \\ a_1 & a_2 & a_3 & a_4 \\ 1 & 0 & 0 & 0 \end{pmatrix} x_0 + \begin{pmatrix} 0 \\ 0 \\ -b_gb_c \\ 0 \end{pmatrix} u_c + \begin{pmatrix} \bar{\Delta}_1 \\ \bar{\Delta}_2 \\ \bar{\Delta}_3 \\ 0 \end{pmatrix}$$

$$y = x_1.$$

The above dynamics has relative degree 3 and is of weak minimum phase since $x_4 = \sigma$ is physically stable. Accordingly, a feedback linearization technique can be applied to the above dynamics and, for easy application, $x = [x_1\ \ \dot{x}_1\ \ \ddot{x}_1\ \ x_4]^T$ is introduced to modify (24) as

$$\dot{x} = \begin{pmatrix} 0 & 1 & 0 & 0 \\ 0 & 0 & 1 & 0 \\ a_1 & a_2 & a_3 & a_4 \\ 1 & 0 & 0 & 0 \end{pmatrix} x + \begin{pmatrix} 0 \\ 0 \\ -b_gb_c \\ 0 \end{pmatrix} u_c + \begin{pmatrix} \Delta_1 \\ \Delta_2 \\ \Delta_3 \\ 0 \end{pmatrix}$$

$$=: a_{igc}x + b_{igc}u_c + \Delta_{igc} \tag{24a}$$

$$y = x_1 \tag{24b}$$

where $\Delta_1 = \bar{\Delta}_1$, $\Delta_2 = \bar{\Delta}_2 + \dot{\bar{\Delta}}_1$, and $\Delta_3 = \bar{\Delta}_3 + \dot{\bar{\Delta}}_2 + \ddot{\bar{\Delta}}_1$.

III. ADAPTIVE NONLINEAR GUIDANCE LAW

In this section, the design procedure of adaptive nonlinear guidance law is presented for the integrated guidance and control system given by (24). The adaptive nonlinear guidance law is designed under the following assumption.

Assumption 1 $|\Delta_i| \le M_i$, and M_i is unknown for $i = 1, 2, 3$.

The guidance law is given by

$$\begin{aligned} u_c = \frac{1}{b_gb_c}\{&a_1x_1 + (a_2 + b_s)\dot{x}_1 + (a_3 + a_s)\ddot{x}_1 + a_4x_4 + ks \\ &+ (b_s\hat{M}_1 + a_s\hat{M}_2 + \hat{M}_3)\mathrm{sgn}(s)\} \end{aligned} \tag{25}$$

and the adaptation law

$$\dot{\hat{M}}_1 = \gamma_1|s|b_s, \qquad \dot{\hat{M}}_2 = \gamma_2|s|a_s, \qquad \dot{\hat{M}}_3 = \gamma_3|s| \tag{26}$$

where $a_s, b_s, k, \gamma_1, \gamma_2, \gamma_3 > 0$ are design parameters, $\hat{M}_i$ is estimate of M_i, $i = 1, 2, 3$, and $s = \ddot{x}_1 + a_s\dot{x}_1 + b_sx_1$ where s-convergence to zero guarantees $\dot{\sigma}$-convergence to zero.

THEOREM 1 (Adaptive nonlinear guidance law) *The missile guidance system described by* (24) *with the guidance law* (25) *and the adaptation law* (26) *under Assumption* 1 *is stable in the sense that*

1) $\tilde{M}_1, \tilde{M}_2, \tilde{M}_3, \hat{M}_1, \hat{M}_2, \hat{M}_3 \in L_\infty$
2) $s, \dot{\hat{M}}_1, \dot{\hat{M}}_2, \dot{\hat{M}}_3 \in L_2 \cap L_\infty$
3) $\dot{s} \in L_\infty$
4) *s, $y(= \dot{\sigma})$, $\dot{\hat{M}}_1$, $\dot{\hat{M}}_2$, and $\dot{\hat{M}}_3$ converges to zero asymptotically.*

PROOF We choose a Lyapunov function

$$V = \frac{1}{2}s^2 + \frac{1}{2\gamma_1}\tilde{M}_1^2 + \frac{1}{2\gamma_2}\tilde{M}_2^2 + \frac{1}{2\gamma_3}\tilde{M}_3^2$$

and take a time derivative to have

$$\begin{aligned}
\dot{V} &= s\dot{s} + \frac{1}{\gamma_1}\tilde{M}_1\dot{\hat{M}}_1 + \frac{1}{\gamma_2}\tilde{M}_2\dot{\hat{M}}_2 + \frac{1}{\gamma_3}\tilde{M}_3\dot{\hat{M}}_3 \\
&= s\{\dddot{x}_1 + a_s\ddot{x}_1 + b_s\dot{x}_1 + (a_s\Delta_2 + b_s\Delta_1)\} \\
&\quad + \frac{1}{\gamma_1}\tilde{M}_1\dot{\hat{M}}_1 + \frac{1}{\gamma_2}\tilde{M}_2\dot{\hat{M}}_2 + \frac{1}{\gamma_3}\tilde{M}_3\dot{\hat{M}}_3 \\
&= s\{a_1x_1 + a_2\dot{x}_1 + a_3\ddot{x}_1 + a_4x_4 - b_gb_cu_c \\
&\quad + a_s\ddot{x}_1 + b_s\dot{x}_1 + (a_s\Delta_2 + b_s\Delta_1 + \Delta_3)\} \\
&\quad + \frac{1}{\gamma_1}\tilde{M}_1\dot{\hat{M}}_1 + \frac{1}{\gamma_2}\tilde{M}_2\dot{\hat{M}}_2 + \frac{1}{\gamma_3}\tilde{M}_3\dot{\hat{M}}_3 \\
&= s\{-ks + (a_s\Delta_2 + b_s\Delta_1 + \Delta_3) \\
&\quad - (b_s\hat{M}_1 + a_s\hat{M}_2 + \hat{M}_3)\mathrm{sgn}(s)\} \\
&\quad + \frac{1}{\gamma_1}\tilde{M}_1\dot{\hat{M}}_1 + \frac{1}{\gamma_2}\tilde{M}_2\dot{\hat{M}}_2 + \frac{1}{\gamma_3}\tilde{M}_3\dot{\hat{M}}_3 \\
&\leq -ks^2 + |s|(a_s\tilde{M}_2 + b_s\tilde{M}_1 + \tilde{M}_3) - \frac{1}{\gamma_1}\tilde{M}_1\dot{\hat{M}}_1 \\
&\quad - \frac{1}{\gamma_2}\tilde{M}_2\dot{\hat{M}}_2 - \frac{1}{\gamma_3}\tilde{M}_3\dot{\hat{M}}_3 \\
&\leq -ks^2.
\end{aligned}$$

Thus, $V(t)$ is bounded for all time, and, accordingly, $s, \tilde{M}_1, \tilde{M}_2, \tilde{M}_3 \in L_\infty$. This yields $\hat{M}_1, \hat{M}_2, \hat{M}_3 \in L_\infty$. Furthermore, as we have $\int_0^\infty s^2(t)dt \leq 1/k\{V(0) - V(\infty)\} < \infty$, $s \in L_2$. From the parameter adaptation law, this means that $\dot{\hat{M}}_1, \dot{\hat{M}}_2, \dot{\hat{M}}_3 \in L_2 \cap L_\infty$. Also, we have $\dot{s} \in L_\infty$. This means that s is uniformly continuous. Combining this with the L_2-property of s, we can use Barbalat's lemma to conclude that s and, accordingly, $y(=\dot{\sigma})$ converge to zero asymptotically. Also, from the parameter adaptation law, $\dot{\hat{M}}_1$, $\dot{\hat{M}}_2$, and $\dot{\hat{M}}_3$ converge to zero asymptotically. □

As the signum term in the guidance law given by (25) and (26) can cause an abrupt change of guidance command, we use the time-varying deadzone using the hyperbolic tangent function [33]. The deadzoned switching surface is defined as

$$s_w = s - \phi_d \cdot \mathrm{sat}(s/\phi_d) \tag{27}$$

where $\mathrm{sat}(\cdot)$ is a saturation function defined by $\mathrm{sat}(a) = \mathrm{sgn}(a)$ for $|a| > 1$ and $\mathrm{sat}(a) = a$ for $|a| \leq 1$, ϕ_d is the width of deadzone with $\phi_d = (1/2(a+bt))\log_e(m_d + 1/m_d - 1)$, and $m_d \neq 1$ and $m_d, a, b > 0$ are design parameters determining the slope of the deadzone around the origin. The guidance law is given by

$$\begin{aligned}
u_c = \frac{1}{b_gb_c}\{&a_1x_1 + (a_2 + b_s)\dot{x}_1 + (a_3 + a_s)\ddot{x}_1 + a_4x_4 \\
&+ ks_w + \mathrm{sat}(s/\phi_d)\cdot m_d(b_s\hat{M}_1 + a_s\hat{M}_2 + \hat{M}_3) \\
&\times \tanh[(a+bt)s] + \dot{\phi}_d\}
\end{aligned} \tag{28}$$

and the adaptation law by

$$\dot{\hat{M}}_1 = \gamma_1|s_w|b_s, \qquad \dot{\hat{M}}_2 = \gamma_2|s_w|a_s, \qquad \dot{\hat{M}}_3 = \gamma_3|s_w|. \tag{29}$$

Stability and performance for the adaptive nonlinear guidance law with time-varying deadzone is shown in the following theorem.

THEOREM 2 (Adaptive nonlinear guidance law with time-varying deadzone) *The missile guidance system described by* (24) *with the guidance law* (28) *and the adaptation law* (29) *under Assumption* 1 *is stable in the sense that*

1) $\tilde{M}_1, \tilde{M}_2, \tilde{M}_3, \hat{M}_1, \hat{M}_2, \hat{M}_3 \in L_\infty$
2) $s_w, \dot{\hat{M}}_1, \dot{\hat{M}}_2, \dot{\hat{M}}_3 \in L_2 \cap L_\infty$
3) $\dot{s}_w \in L_\infty$
4) *s, $\dot{\sigma}$, $\dot{\hat{M}}_1$, $\dot{\hat{M}}_2$, and $\dot{\hat{M}}_3$ converges to zero asymptotically.*

PROOF We choose a Lyapunov function

$$V = \frac{1}{2}s_w^2 + \frac{1}{2\gamma_1}\tilde{M}_1^2 + \frac{1}{2\gamma_2}\tilde{M}_2^2 + \frac{1}{2\gamma_3}\tilde{M}_3^2.$$

For $|s| \leq \phi_d$, we have $\dot{V} = 0$ using $s_w = 0$. For $|s| > \phi_d$, we use $\dot{s}_w = \dot{s} - \dot{\phi}_d$ to have

$$\begin{aligned}
\dot{V} &= s_w\dot{s}_w + \frac{1}{\gamma_1}\tilde{M}_1\dot{\hat{M}}_1 + \frac{1}{\gamma_2}\tilde{M}_2\dot{\hat{M}}_2 + \frac{1}{\gamma_3}\tilde{M}_3\dot{\hat{M}}_3 \\
&= s_w\{\dddot{x}_1 + a_s\ddot{x}_1 + b_s\dot{x}_1 + (a_s\Delta_2 + b_s\Delta_1) - \dot{\phi}_d\} \\
&\quad + \frac{1}{\gamma_1}\tilde{M}_1\dot{\hat{M}}_1 + \frac{1}{\gamma_2}\tilde{M}_2\dot{\hat{M}}_2 + \frac{1}{\gamma_3}\tilde{M}_3\dot{\hat{M}}_3.
\end{aligned}$$

Using the third row of (24a), this becomes

$$\begin{aligned}
\dot{V} = s_w\{&a_1x_1 + a_2\dot{x}_1 + a_3\ddot{x}_1 + a_4x_4 - b_gb_cu_c \\
&+ a_s\ddot{x}_1 + b_s\dot{x}_1 + (a_s\Delta_2 + b_s\Delta_1 + \Delta_3) - \dot{\phi}_d\} \\
&- \frac{1}{\gamma_1}\tilde{M}_1\dot{\hat{M}}_1 - \frac{1}{\gamma_2}\tilde{M}_2\dot{\hat{M}}_2 - \frac{1}{\gamma_3}\tilde{M}_3\dot{\hat{M}}_3.
\end{aligned}$$

Using the guidance law (28) and the adaptation law (29) and using $\mathrm{sat}(s/\phi_d) = \mathrm{sgn}(s_w)$ for $|s| > \phi_d$, we have

$$\begin{aligned}
\dot{V} \leq\ & -ks_w^2 + |s_w|(b_sM_1 + a_sM_2 + M_3) - \frac{1}{\gamma_1}\tilde{M}_1\dot{\hat{M}}_1 \\
& - \frac{1}{\gamma_2}\tilde{M}_2\dot{\hat{M}}_2 - \frac{1}{\gamma_3}\tilde{M}_3\dot{\hat{M}}_3 \\
& - |s_w|m_d(b_s\hat{M}_1 + a_s\hat{M}_2 + \hat{M}_3)\tanh[(a+bt)s]
\end{aligned}$$

$$\leq -ks_w^2 + |s_w|(b_s\tilde{M}_1 + a_s\tilde{M}_2 + \tilde{M}_3) - \frac{1}{\gamma_1}\tilde{M}_1\dot{\hat{M}}_1 - \frac{1}{\gamma_2}\tilde{M}_2\dot{\hat{M}}_2 - \frac{1}{\gamma_3}\tilde{M}_3\dot{\hat{M}}_3 + |s_w|(b_s\hat{M}_1 + a_s\hat{M}_2 + \hat{M}_3) - |s_w|m_d(b_s\hat{M}_1 + a_s\hat{M}_2 + \hat{M}_3)\tanh[(a+bt)|s|]$$
$$= -ks_w^2 + |s_w|(b_s\hat{M}_1 + a_s\hat{M}_2 + \hat{M}_3) \times \{1 - m_d \tanh[(a+bt)|s|]\}.$$

For $|s| > \phi_d$, it follows that

$$\dot{V} \leq -ks_w^2 + |s_w|(b_s\hat{M}_1 + a_s\hat{M}_2 + \hat{M}_3) \times \{1 - m_d \tanh[(a+bt)\phi_d]\}$$
$$= -ks_w^2 + |s_w|(b_s\hat{M}_1 + a_s\hat{M}_2 + \hat{M}_3) \times \left\{1 - m_d \tanh\left[\frac{1}{2}\log_e\left(\frac{m_d+1}{m_d-1}\right)\right]\right\}.$$

Now we use the relation

$$\tanh(x) = \frac{e^x - e^{-x}}{e^x + e^{-x}} = \frac{e^{2x}-1}{e^{2x}+1}$$

to have

$$\dot{V} \leq -ks_w^2 + |s_w|(b_s\hat{M}_1 + a_s\hat{M}_2 + \hat{M}_3) \times \left\{1 - m_d\frac{(m_d+1)-(m_d-1)}{(m_d+1)+(m_d-1)}\right\}$$
$$= -ks_w^2.$$

Thus, $V(t)$ is bounded for all time and, accordingly, $s_w, \tilde{M}_1, \tilde{M}_2, \tilde{M}_3 \in L_\infty$. This directly yields $\hat{M}_1, \hat{M}_2, \hat{M}_3 \in L_\infty$. Furthermore, we can easily check that $s_w \in L_2$ and with the parameter adaptation law $\dot{\hat{M}}_1, \dot{\hat{M}}_2, \dot{\hat{M}}_3 \in L_2 \cap L_\infty$. Also, we have $\dot{s}_w \in L_\infty$. This means that s_w is uniformly continuous. Combining this with the L_2-property of s_w, we can use Barbalat's lemma to conclude that s_w, together with $\dot{\hat{M}}_1, \dot{\hat{M}}_2, \dot{\hat{M}}_3$, converge to zero asymptotically. This, in turn, guarantees that $|s| \leq \phi_d$ holds after some time. As $\lim_{t\to\infty} |\phi_d| = 0$ holds, we also have $\lim_{t\to\infty} |s| = 0$. □

REMARK 1 As ϕ_d goes to zero with time, the adaptive guidance law with deadzone, that is (28) and (29), becomes the same as the one without deadzone, that is (25) and (26), in Theorem 1. Thus, using a saturation function and time-varying deadzone in the adaptive guidance law, we can guarantee the performance of $\dot{\sigma}$-convergence to zero and the stability of the overall system without incurring the high frequency inputs.

IV. SIMULATION RESULTS

This section presents simulation results for the proposed adaptive nonlinear guidance (ANG) law for yaw and pitch dynamics. The ANG law (28), (29) is slightly modified in the simulation mainly from the implementation considerations using $R^{(3)} \approx R^{(4)} \approx 0$ as in [27]. Note that a hyperbolic tangent function is used in a guidance law instead of a signum function. The former function is differentiable and adopts a time varying deadzone, whereas the latter adopts a fixed deadzone. As the missile reaches the end-game phase, the performance, such as the minimization of miss distance and flight time, is more important than the stability of the missile system. Thus, the proposed system focuses on the performance, considering the more realistic situation.

The performance of the proposed law is evaluated for a missile-target interception in a more realistic situation. The simulation has been done for surface-to-air engagement scenarios, which depend on the conditions of the missile and the target. The performance of the proposed method is compared with that of the proportional navigation guidance (PNG) law, augmented PNG (APNG) law, and sliding mode guidance (SMG) law. Each of the PNG, APNG, SMG guidance laws are of the form

$$u_{PNG} = NV_c\dot{\sigma} = \frac{N}{t_{go}^2}(y_R + \dot{y}_R t_{go}) \tag{30}$$

$$u_{APNG} = \frac{N}{t_{go}^2}(y_R + \dot{y}_R t_{go} + 0.5a_{T\gamma}t_{go}^2) \tag{31}$$

$$u_{SMG} = (N+1)V_c\dot{\sigma} + \varepsilon_s\frac{\dot{\sigma}}{|\dot{\sigma}| + \delta_s} \tag{32}$$

where N is a navigation constant chosen as 3, V_c is closing velocity, t_{go} is time-to-go, $a_{T\gamma}$ is target acceleration at the γ-axis (either the x-y or the x-z plane), and ε_s and δ_s are 1 and 0.05, respectively. The miss distance and flight time are chosen as performance indices. The actual missile control system in [31] is employed in a closed-loop guidance and control simulation environment described in [32], making the evaluation more practical. Design parameters of the control loop (3) are $\xi = 0.7$ and $\omega_n = 15$. Design parameters of guidance loop (28), (29), and ϕ_d are $a_s = 250$, $b_s = 1$, $k = 20$, $m_d = 2$, $\gamma_1 = 0.1$, $\gamma_2 = 0.1$, $\gamma_3 = 0.1$, $a = 0.1$, and $b = 0.2$.

Here, we select several scenarios shown in Table I. We conduct simulations for various other scenarios as well and find that the proposed system is effective in most cases. In these scenarios, the target initially travels at constant velocity with 200 m/s, then makes step-changes in acceleration. Each vector component in Table I represents the value along the y and z axes, respectively. The launch angle, elevation angle, azimuth angle, and control start time of the missile are 50 deg, 0 deg, 0 deg, and 0.5 s, respectively.

Fig. 2 shows the acceleration tracking performance and three-dimensional trajectories of PNG and ANG for scenario I in Table I. Table II compares the miss distances and flight time of PNG, APNG, SMG,

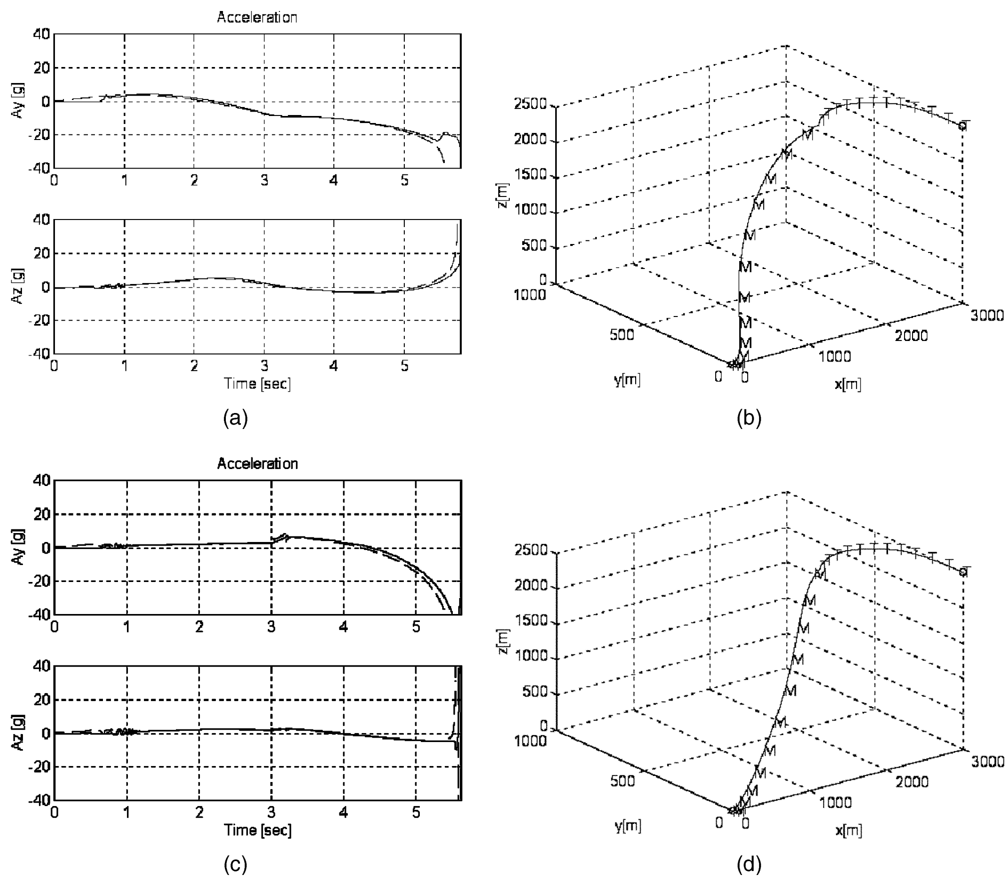

Fig. 2. Performance of scenario I. (a) Acceleration of PNG. (b) Three-dimensional trajectory of PNG. (c) Acceleration of ANG. (d) Three-dimensional trajectory of ANG. In (a) and (c), solid is actual acceleration and dotted is acceleration command. In (b) and (d), M is missile, T is target.

TABLE I
Scenarios for Missile-Target Interception

(a) Target Conditions

Scenario	First Evasive Time (s)	First Evasive Acceleration (m/s^2)	Second Evasive Time (s)	Second Evasive Acceleration (m/s^2)
I	0	[0 8]	2	[−8 0]
II	0	[4 −4]	2	[8 −8]
III	0	[0 −10]	2.5	[15 0]
IV	0	[0 0]	0	[0 0]
V	0	[0 0]	0	[0 0]
VI	0	[0 7]	1	[7 −7]
VII	1	[10 −10]	4	[−10 10]
VIII	0	[10 −20]	7	[0 0]

(b) Target-Missile Geometry

Scenario	Off-Boresight Angle (deg)	Aspect Angle (deg)	Initial Relative Distance (m)	Initial Relative Altitude (m)
I	0	90	3000	2500
II	−30	−90	2000	1300
III	45	180	1500	1000
IV	0	0	300	1500
V	0	180	2000	1000
VI	0	180	1500	1300
VII	0	45	2000	1000
VIII	0	−30	2000	1000

TABLE II
Performance of PNG, APNG, SMG, and ANG without Uncertainties

(a) Miss Distance (m)

Scenario	PNG	APNG	SMG	ANG
I	4.3244	12.5096	0.6199	0.3164
II	7.7048	3.2928	1.0344	4.0061
III	1.8637	2.0831	0.8709	0.3257
IV	1.0499	1.0499	0.4395	0.1978
V	6.5488	6.5488	5.4528	0.0896
VI	1.1949	1.0524	0.8112	0.2071
VII	2.0209	15.1730	0.5119	1.3549
VIII	83.818	181.3973	63.5237	44.612

(b) Flight Time (s)

Scenario	PNG	APNG	SMG	ANG
I	5.8085	6.0720	5.8420	5.6490
II	4.9505	5.1545	5.0325	4.8155
III	3.9255	3.7610	3.9425	3.7280
IV	3.7500	3.7500	3.7570	3.6580
V	2.0940	2.0940	2.0950	2.0775
VI	3.3790	3.4255	3.3795	3.3720
VII	5.3660	7.0010	5.4345	5.3110
VIII	4.8450	7.0080	4.9000	4.6845

TABLE III
Performance of PNG, APNG, SMG, and ANG with Uncertainties

(a) Miss Distance (m)				
Scenario	PNG	APNG	SMG	ANG
I	18.894	101.0000	15.3689	10.3333
II	104.08	178.7423	89.0944	13.4023
III	12.825	23.6034	9.7647	2.4559
IV	4.4769	4.4769	2.5142	0.2041
V	9.9751	9.9751	8.9779	0.1065
VI	1.5034	1.7627	2.1903	0.2171
VII	16.470	446.0893	19.9431	13.828
VIII	179.00	76.4673	171.7629	65.384
(b) Flight Time (s)				
Scenario	PNG	APNG	SMG	ANG
I	5.9420	6.3925	5.9720	5.6895
II	5.0645	5.5805	5.3670	4.9125
III	4.1475	3.8645	4.1715	3.7485
IV	3.7805	3.7805	3.8020	3.6640
V	2.0885	2.0885	2.0885	2.0790
VI	3.3900	3.4795	3.3925	3.3825
VII	5.5765	7.0010	5.7080	5.4580
VIII	4.8855	5.3905	4.9385	4.6445

and ANG under each scenario. The results in Fig. 2 show that the acceleration commands and also the actual acceleration become different between PNG and ANG. This difference results in the smaller miss distance and flight time with ANG than with PNG as shown in Table II. It should be noted that PNG, APNG, and SMG do not consider the actual control loop response and thus show much degraded performance compared with ANG for severe target maneuver.

The advantage of the proposed method becomes more apparent against uncertainties in the missile dynamics. We assume as in [34] that uncertainties exist in $C_y(M_m,\beta,\delta_r,\phi_A)$ and $C_z(M_m,\alpha,\delta_q,\phi_A)$ as

$$C_y(M_m,\beta,\delta_r,\phi_A) = C_{yn}(M_m,\beta,\delta_r,\phi_A) + \vartheta_{fy}^T\phi_{fy}$$
$$C_z(M_m,\alpha,\delta_q,\phi_A) = C_{zn}(M_m,\alpha,\delta_q,\phi_A) + \vartheta_{fz}^T\phi_{fz}$$

where $C_{yn}(M_m,\beta,\delta_r,\phi_A)$ and $C_{zn}(M_m,\alpha,\delta_q,\phi_A)$ are nominal values given by aerodynamic coefficient table, ϕ_{fy} and ϕ_{fz} are variables corresponding to ϕ_f, $\phi_f^T = [\phi_{f1}^T,\ldots,\phi_{fN}^T]$, $\phi_{fi}^T = [\phi_{fi1}\ \ \phi_{fi2}\ \ \phi_{fi3}\ \ \phi_{fi4}] = \mu_i(M_m)[\beta\ \ \beta\sin^2(2\phi_A)\ \ \beta^3\ \ \beta^3\sin^2(2\phi_A)]$, and ϑ_{fy} and ϑ_{fz} are uncertain parameters given by

$$\vartheta_{fy1}^T = [0.5\quad 10],\qquad \vartheta_{fy2}^T = [4.5\quad 15],\qquad \vartheta_{fy3}^T = [2.6\quad 35]$$
$$\vartheta_{fy4}^T = [2.0\quad 27],\qquad \vartheta_{fy5}^T = [3.6\quad 37],\qquad \vartheta_{fy6}^T = [3.2\quad 25]$$
$$\vartheta_{fz1}^T = [3.5\quad 20],\qquad \vartheta_{fz2}^T = [2.4\quad 24],\qquad \vartheta_{fz3}^T = [3.5\quad 10]$$
$$\vartheta_{fz4}^T = [3.4\quad 32],\qquad \vartheta_{fz5}^T = [4.4\quad 17],\qquad \vartheta_{fz6}^T = [1.3\quad 22].$$

In this case, the results of the proposed guidance law and also those of PNG, APNG, and SMG are compared in Table III and it can be confirmed that the proposed one can effectively compensate for the uncertainties in control loop dynamics. The results show that the proposed scheme can be effectively combined with the previously developed missile control system, forming the integrated guidance and control system.

V. CONCLUSIONS

We proposed an adaptive nonlinear guidance law to improve the overall performance of guidance and control missile system. The proposed approach, when compared with the existing results, is novel in that the guidance law considers the uncertainties of control dynamics as well as target acceleration. In addition, stability analysis has been provided for the overall system including the guidance and control loop. The simulation results as well as the stability and performance analysis show that our scheme can be effectively used to improve the overall guidance and control system.

ACKNOWLEDGMENTS

The authors would like to thank Jinho Kim, Chanho Song, Hangju Cho, and In-Joong Ha for their valuable comments, and Heum-Pil Cho and Jun-ho Kang for their assistance in simulations.

REFERENCES

[1] Pastric, H. J., Setlzer, S., and Warren, M. E. (1981)
Guidance laws for short range homing missile.
Journal of Guidance, Control, and Dynamics, **4**, 2 (1981), 98–108.

[2] Cloutier, J. R., Evers, J. H., and Feeley, J. J. (1989)
Assessment of air to air missile and guidance technology.
IEEE Control Systems Magazine, **9**, 6 (Oct. 1989), 27–34.

[3] Murtaugh, S. A., and Criel, H. E. (1966)
Fundamentals of proportional navigation.
IEEE Spectrum, **3**, 6 (1966), 75–85.

[4] Guelman, M. (1976)
The closed form solution of true proportional navigation.
IEEE Transactions on Aerospace and Electronic Systems, **AES-12**, 4 (1976), 472–482.

[5] Zarchan, P. (1990)
Tactical and Strategic Missile Guidance.
Progress in Aeronautics and Astronautics, 1990.

[6] Siouris, G. M. (1974)
Comparison between proportional and augmented proportional navigation.
Nachritentechnische Zeitschrift, (July 1974), 278–280.

[7] Bryson, A. E., and Ho, Y. C. (1975)
Applied Optimal Control.
New York: Hemisphere Publishing, 1975.

[8] Lin, C. F. (1992)
Modern Navigation, Guidance, and Control Processing.
Englewood Cliffs, NJ: Prentice-Hall, 1992.

[9] Yang, C. D., and Yeh, F. B. (1988)
Optimal proportional navigation.
Journal of Guidance, Control, and Dynamics, **11**, 4 (1988), 375–377.

[10] Asher, R. B., and Martuszewski, J. P. (1974)
Optimal guidance with maneuvering targets.
Journal of Spacecraft and Rockets, **11**, 3 (1974), 204–206.

[11] Cottrel, R. G. (1971)
Optimal intercept guidance for short range tactical missiles.
AIAA Journal, **9**, 7 (1971), 1414–1415.

[12] Nesline, F. W., and Zarchan, P. (1981)
A new look at classical versus modern homing missile guidance.
Journal of Guidance, Control, and Dynamics, **4**, 1 (1981), 78–85.

[13] Holder, E. J., and Sylvester, V. B. (1990)
An analysis of modern versus classical homing guidance.
IEEE Transactions on Aerospace and Electronic Systems, **26**, 4 (July 1990), 599–606.

[14] Rusnak, I., and Meir, L. (1991)
Modern guidance law for high-order autopilot.
Journal of Guidance, Control, and Dynamics, **14**, 3 (1991), 1056–1058.

[15] Yuan, P. J., and Chern, J. S. (1992)
Ideal proportional navigation.
Journal of Guidance, Control, and Dynamics, **15**, 5 (1992), 1161–1166.

[16] Yang, C. D., Yeh, F. B., and Chen, J. H. (1987)
The closed form solution of generalized proportional navigation.
IEEE Transactions on Aerospace and Electronic Systems, **AES-10**, 2 (1987), 216–218.

[17] Yang, C. D., Yeh, F. B., and Hsiao, F. B. (1989)
Generalized guidance law for homing missiles.
IEEE Transactions on Aerospace and Electronic Systems, **25**, 2 (1989), 197–212.

[18] Cochran, J. E., No, T. S., and Thaxton, D. G. (1991)
Analytic solutions to a guidance problem.
Journal of Guidance, Control, and Dynamics, **14**, 1 (1991), 117–122.

[19] Yuan, P. J., and Chern, J. S. (1992)
Solutions of true proportional navigation for maneuvering and nonmaneuvering targets.
Journal of Guidance, Control, and Dynamics, **15**, 1 (1992), 268–271.

[20] Song, S. H., and Ha, I. J. (1994)
A Lyapunov-like approach to performance analysis of 3-dimensional pure PNG laws.
IEEE Transactions on Aerospace and Electronic Systems, **30**, 1 (1994), 238–247.

[21] Bezik, S., Rusnak, I., Gray, W. S. (1995)
Guidance of a homing missile via nonlinear geometric control methods.
Journal of Guidance, Control, and Dynamics, **18**, 3 (1995), 441–448.

[22] Ha, I. J., and Chong, S. (1992)
Design of a CLOS guidance law via feedback linearization.
IEEE Transactions on Aerospace and Electronic Systems, **28**, 1 (1992), 51–62.

[23] Huang, J., and Lin, C. F. (1995)
A modified CLOS guidance law via right inversion.
IEEE Transactions on Aerospace and Electronic Systems, **31**, 1 (1995), 491–495.

[24] Yang, C. D., and Chen, H. Y. (1998)
Nonlinear H_∞ robust guidance law for homing missiles.
Journal of Guidance, Control, and Dynamics, **21**, 6 (1998), 882–890.

[25] Brierley, S. D., and Longchamp, R. (1990)
Application of sliding mode control to air-air interception problem.
IEEE Transactions on Aerospace and Electronic Systems, **26**, 2 (1990), 306–325.

[26] Babu, K. R., Sarma, I. G., and Swamy, K. N. (1994)
Switched bias proportional navigation for homing guidance against highly maneuvering target.
Journal of Guidance, Control, and Dynamics, **17**, 6 (1994), 1357–1363.

[27] Zhou, D., Mu, C., and Xu, W. (1999)
Adaptive sliding-mode guidance of a homing missile.
Journal of Guidance, Control, and Dynamics, **22**, 4 (1999), 589–594.

[28] Lin, C. F., Wang, Q., Speyer, J. L., Evers, J. H., and Cloutier, J. R. (1992)
Integrated estimation, guidance, and control system design using game theoretic approach.
In *Proceedings of the American Control Conference*, Chicago, IL, 1992, 3220–3224.

[29] Evers, J. H., Cloutier, J. R., Lin, C. F., Yueh, W. R., and Wang, Q. (1992)
Application of Integrated guidance and control schemes to a precision guided missile.
In *Proceedings of the American Control Conference*, Chicago, IL, 1992, 3225–3230.

[30] Lin, C. F., Ohlmeyer, E., Bibel, J. E., and Malyevac, S. (1998)
Optimal design of integrated missile guidance and control.
Presented at the 1998 World Aviation Conference, Anaheim, CA, Sept. 1998, AIAA-985519.

[31] Chwa, D. and Choi, J. Y. (2001)
New parametric affine modeling and control for skid-to-turn missiles.
IEEE Transactions on Control Systems Technology, **9**, 2 (Mar. 2001), 335–347.

[32] Choi, J. Y., Chwa, D., and Kim, M. S. (2000)
Adaptive control for feedback-linearized missiles with uncertainties.
IEEE Transactions on Aerospace and Electronic Systems, **36**, 2 (Apr. 2000), 467–481.

[33] Song, G., and Mukherjee, R. (1998)
A comparative study of conventional non-smooth time-invariant and smooth time-varying robust compensators.
IEEE Transactions on Control Systems Technology, **6**, 4 (1998), 571–576.

[34] Choi, J. Y., and Chwa, D. (2000)
Adaptive control based on a parametric affine model for tail-controlled missiles.
In *Proceedings of the 39th IEEE Conference on Decision and Control*, Sydney, Dec. 2000, 1471–1476.

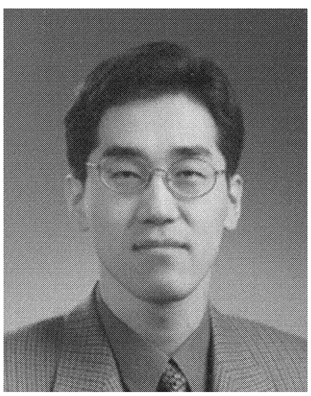

Dongkyoung Chwa (S'89—M'93) received the B.S. and M.S. degrees in control and instrumentation engineering in 1995 and 1997, respectively, and Ph.D. degree from the School of Electrical Engineering and Computer Science in 2001, all from Seoul National University, Seoul, Korea.

From 2001 to 2003, he was a post-doctoral researcher at Seoul National University. In 2003, he was a visiting research fellow at the UNSW@ADFA (The University of New South Wales at Australian Defence Force Academy) and the Honorary Visiting Academic at the University of Melbourne, all in Australia. Since 1995, he has been affiliated with the Automatic Control Research Center (ACRC) in Seoul National University. His research interests are nonlinear, robust, and adaptive control theories, and their applications to the missile guidance and control, robotics, and nonlinear flight systems.

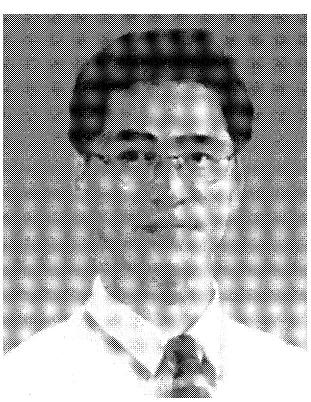

Jin Young Choi (S'89—M'93) received the B.S., M.S., and Ph.D. degrees in control and instrumentation engineering from Seoul National University, Seoul, Korea, in 1982, 1984, and 1993, respectively.

From 1984 to 1989, he was with the Electronics and Telecommunication Research Institute (ETRI). From 1992 to 1994, he was with the Basic Research Department of ETRI, where he was a senior member of technical staff working on the neural information system. Since 1994, he has been with Seoul National University, where he is currently an assistant professor in the School of Electrical Engineering. He is also affiliated with Automation and Systems Research Institute (ASRI), Engineering Research Center for Advanced Control and Instrumentation (ERC-ACI), and Automatic Control Research Center (ACRC) at Seoul National University. From 1998 to 1999, he was visiting professor at the University of California, Riverside. His research interests are neuro computing and control, evolutionary computing, adaptive and learning control, and their applications to missile, nuclear power plant, rapid thermal processing systems, and motors.